Charge Density Effect of Polyelectrolyte Chains on the Nanostructures of Polyelectrolyte−Surfactant Complexes

Shuiqin Zhou,† Christian Burger,‡ Fengji Yeh,† and Benjamin Chu*,†

Department of Chemistry, State University of New York at Stony Brook, Stony Brook, New York 11794-3400, and Max-Planck-Institut für Kolloid- & Grenzflächenforschung, Kantstrasse 55, D-14513 Teltow-Seehof, Germany

Received June 26, 1998

ABSTRACT: Small-angle X-ray scattering was used to investigate the nanostructures of complexes formed by slightly cross-linked anionic copolymer gels of poly(sodium methacrylate-*co*-*N*-isopropylacrylamide) P(MAA/NIPAM) interacting with tetradecyltrimethylammonium bromide (TTAB), and dodecyltrimethylammonium bromide (DTAB), respectively, at room temperature (∼23 °C). In sequence with decreasing charge density of the P(MAA/NIPAM) copolymer chains, the structures of *Pm*3*n* space group cubic, face-centered cubic close packing of spheres, and hexagonal close packing of spheres were respectively determined. The structural elements of spheres and/or rods were shown to be the spherical and/or cylindrical micelles formed by the self-assembly of TTA or DTA cations driven by both electrostatic and hydrophobic interactions of the charged copolymer chains/surfactants and of the surfactants/surfactants inside the polyelectrolyte gel matrix. Both the aggregation number and the size of the micelles decreased with decreasing charge density of the copolymer chains. By further decreasing the charge density of the P(MAA/NIPAM) chains, the structures of resulting complexes became less ordered.

Introduction

The interactions between polyelectrolyte and oppositely charged amphiphiles have attracted special interest in the last two decades, due both to its importance in fundamental polymer physics/biophysics as well as in industrial applications. The biological significance stems from the fact that many biomacromolecules, such as the various polynucleic acids and proteins are polyelectrolytes and various lipids are surfactants. The use of cationic liposomes in the transfer of genes has become a popular method of gene therapy.[1−4] The interactions of polyelectrolytes with oppositely charged surfactants are quite strong and can induce complex formation with highly ordered structures. These ordered structures have a host of possible applications ranging from improved mechanical behavior to unusual optical, electrical, and biological properties.[5] Both electrostatic interactions between charged components as well as hydrophobic interactions between the polymer backbone and the alkyl tail of the surfactant are important in driving the self-assembly of surfactant molecules to form ordered structures inside the complexes.[6−10]

Surfactants in water exhibit very rich and complex self-organized structures that are the basis of the structure-forming abilities of the polyelectrolyte−surfactant complexes.[5] In comparison with the rich phase structures of molecular organizations in binary mixtures constructed from water and surfactants,[11−16] far too little is known about the phase structures of the polyelectrolyte−surfactant complexes. The structure of the polyelectrolyte−surfactant complexes depends greatly on the competition between the rate of complex formation and the rate by which a thermodynamically equilibrated complex phase is eventually formed. Some structures that are the same as in surfactant/water binary system should be observable in polyelectrolyte−surfactant complexes. In the meantime, threading polyelectrolyte chains through these mesophases may also create different geometrical constraints from surfactants, thus producing some new structures. It could be expected that the charge density of the polyelectrolyte chains would significantly affect the structures of the complexes.

Substantial efforts have been made to clarify the structures of polyelectrolyte−surfactant complexes in the last five years.[9,17−24] Kabanov et al.[17] reported a lamellar structure for complexes of poly(sodium acrylate) gel−alkyltrimethylammonium bromide. Okuzaki and Osada[9] proposed a simple cubic structure for the complexes formed by poly(2-(acrylamido)-2-methylpropanesulfonic acid) (PAMPS) and alkylpyridinium chloride (APCl). Antonietti et al.[19−23] have studied the solid-state structures of various polyelectrolyte−surfactant complexes. A structure of face-centered cubic packing of undulated cylinders was proposed for the complex of poly(sodium acrylate)−dodecyltrimethylammonium. Different undulated lamellar structures were proposed for complexes of polystyrenesulfonate−alkyltrimethylammonium salts. They also made complexes by the interactions between copolymers of poly(acrylate-*co*-tetradecylacrylamide) [P(AA/TDAA)] or poly[(sodium 2-acrylamido-2-methyl-1-propanesulfonate)-*co*-octadecylacrylamide] [P(AMPS/ODAA)] with cetyltrimethylammonium salt (CTA).[21] Depending on the copolymer compositions, lamellar, modulated-lamellar, hexagonal packing of cylinders, and bicontinuous sponge phase structures were observed, respectively, in the P(AA/TDAA)−CTA and P(AMPS/ODAA)−CTA complexes. Very recently, the Ober group[5] suggested a lamellar structure for the poly(methacrylate) (PMAA)−CTA complex. It could be seen that most of the polyelectrolyte−surfactant complexes studied so far showed lamellar, cylindrical, and undulating layered structures. Moreover, some strcutures described above might be ill-identified due to the poor resolution of X-ray scattering curves.

In our laboratory in the past few years, synchrotron small-angle X-ray scattering (SAXS) has been used to

10.1021/ma9810058 CCC: $15.00
Published on Web 10/31/1998

investigate the structures of the complexes formed by cationic gels of poly(diallyldimethylammonium chloride)(PDADMACl) interacting with anionic surfactants of sodium alkyl-sulfate (SC_nS).[18,24] Hexagonal packing of cylinders for complexes of PDADMACl−SC_nS at $n \geq 12$ and cubic structures for complexes of PDADMACl−SC_nS at $n \leq 10$ were observed, respectively. However, the cubic structure was not analyzed, and the charge contents of the copolymer chains were not quantitatively controlled as desired due to the large difference in the reactivity ratio between the DADMACl cationic monomer and acrylamide neutral comonomer.

In this paper, we have chosen *N*-isopropylacrylamide (NIPAM) as a neutral comonomer to be copolymerized with sodium methacrylate (MAA) anionic monomer to produce the slightly cross-linked negatively charged polyelectrolyte hydrogel. The desired charge content could be controlled because of the similar reactivity ratio of component i (r_i) for the two comonomers, namely, $r_1 = 0.89$ for NIPAM and $r_2 = 1.13$ for MAA, respectively.[25] Tetradecyltrimethylammonium bromide (TTAB) and dodecyltrimethylammonium bromide (DTAB) have been used as cationic surfactants to produce complexes. The objectives of the present paper are to study the charge density effect of polyelectrolyte network chains on the phase structures of the formed complexes and to analyze the novel phase structures observed in P(MAA/NIPAM) gel−TTA and −DTA complexes. Structures of $Pm3n$ space group cubic, face-centered cubic close packing of spheres, hexagonal close packing of spheres were, for the first time, observed in polyelectrolyte−surfactant complexes.

Experimental Section

Materials. Methacrylic acid (MAA) monomer (Aldrich, 98.5%) was vacuum distilled. NIPAM monomer (ARCOS, 99%) was purified by recrystallization in a toluene/hexane mixture. *N*,*N*′-Methylenebis(acrylamide) (BIS) (Ultragrade, Pharmacia LKB) as a cross-linker, and ammonium persulfate (APS) (Aldrich, 98+%) as an initiator, were used as received. The surfactants of TTAB (Lancaster, 98%) and DTAB (Fluka, ≥98%) were used without further purification. Deionized water was distilled before use.

Gel Preparation. Gels were prepared by free radical copolymerization. A 15 wt % aqueous solution (5−8 mL) of a reaction mixture with a desired comonomer molar ratio and a cross-linker density of 1 mol % (of total monomers) was bubbled with nitrogen for 15 min to remove oxygen in the reaction mixture. Then 35 μL of a 10 wt % APS solution was added to the mixture. The final solutions were filtered through a 0.22 μm Millipore filter and injected into the space between two glass plates separated by two spacers with a thickness of 0.63 ± 0.04 mm. Gelation was carried out at 65 °C for 24 h. One portion of the resulting gels was washed in distilled deionized water to remove the unreacted monomers and was titrated with aqueous sodium hydroxide solution to determine the composition of the copolymer. Another portion of the gels was washed in a large amount of dilute sodium hydroxide solution for 3 weeks in order to neutralize the poly(methacrylic acid) and to remove the unreacted monomers. The dilute sodium hydroxide solution was changed every 1−2 days, and the final pH value was kept at ∼8.2.

P(MAA/NIPAM) Gel−Surfactant Complexation. Complexes were prepared by immersing known amounts of neutralized and water *swollen* gel disks (10 mm diameter, 2−3 mm thick) in a very dilute aqueous sodium hydroxide solution of surfactants (pH ∼8−9). The surfactant concentration was approximately one-third of the critical micelle concentration (CMC) for the corresponding surfactant in the external solution phase. The total volume of the surfactant solution was controlled at such a level that the ratio r, defined by ⟨number of surfactant molecules in solution⟩/⟨number of charged groups in the polymer networks⟩, was in the range of $r \geq 2$. It means that the number of surfactant molecules was always in excess of the number of charged groups in the copolymer chain for complexation. The gel disks were equilibrated in the surfactant solution for about 4 weeks before being taken out for SAXS measurements. In addition, the equilibrated gel−surfactant complexes were also washed on the surface by water, and vacuum-dried to determine the compositions of the dried complexes by elemental analysis (M-H-W Lab, AZ). No bromine was detectable inside the complexes.

X-ray Scattering Measurements. SAXS measurements were performed at the X3A2 State University of New York Beam Line, National Synchrotron Light Source at Brookhaven National Laboratory, using a laser-aided prealigned pinhole collimator.[26] The incident beam wavelength (λ) was tuned at 0.154 nm. A 2D detector imaging plate was used in conjunction with an image scanner manufactured by Fujitsu Co. as the detection system. The sample to detector distance was 787 mm, corresponding to a q range of $0.2 \leq q \leq 4.8$ nm^{-1} with $q = (4\pi/\lambda)\sin(\theta/2)$ and θ being the scattering angle between the incident and the scattered X-rays. The experimental data were corrected for background scattering and sample transmission. The smearing effect was negligible for this setup.

Results and Discussion

The P(MAA/NIPAM) gel underwent a volume contraction when placed in the TTAB or DTAB solution. Depending on the charge content of polyelectrolyte chains, the surfactant solution concentration, and the tail properties of the surfactant, the gels showed different collapse kinetics and various degrees of collapse. Typically, the P(MAA/NIPAM) gels reached an equilibrium state of collapse after 3 weeks in TTAB solution, and 2 weeks in DTAB solution, respectively. The elemental analysis results showed that the complex formation was essentially a stoichiometric binding reaction of the surfactant molecules with the copolymer network chains in terms of charges. Accordingly, there could only be slightly cross-linked negatively charged PMAA or P(MAA/NIPAM) chains, TTA or DTA cations, and water inside the complexes after the gels reached the equilibrium of collapse. By knowing the weight of the dried gel [poly(sodium methacrylate/NIPAM) chains] before complexation, the weight of complexes equilibrated with water (the water on the surface of complex disks was adsorbed before weighing), and the weight of the dried complexes, we could determine the weight fraction of P(MAA/NIPAM) chains, TTA or DTA cations, and water inside the complexes. Table 1 lists the compositions of some P(MAA/NIPAM) gel−TTA or −DTA complexes.

I. P(MAA/NIPAM)−TTA Systems. A. *Pm3n* Cubic Structure. Figure 1 shows a typical SAXS profile of the PMAA gel−TTA complex formed with fully

Table 1. Compositions and Structure Parameters of Partial P(MAA/NIPAM) Gel−TTA and P(MAA/NIPAM) Gel−DTA Complexes[a]

complexes/charge density	structure	composition[a]	dimension of unit cell/nm	R_{sph}/nm	R_{lit}/nm	N_{agg}	N_{lit}
gel−TTA/67 mol %	FCC	$\phi_{TTA} = 0.38$ $\phi_p = 0.18$ $\phi_w = 0.44$	$a = 7.0$	2.0	2.4	63	66 (TTACl) 68 (TTABr)
gel−TTA/50 mol %	HCP	$\phi_{TTA} = 0.35$ $\phi_p = 0.22$ $\phi_w = 0.43$	$a = 4.8$ $b = 8.4$ $c = 7.9$	1.9		53	
gel−DTA/75 mol %	HCP	$\phi_{DTA} = 0.37$ $\phi_p = 0.16$ $\phi_w = 0.47$	$a = 4.5$ $b = 7.8$ $c = 7.4$	1.8	2.1	52	47 (DTACl)
gel−DTA/67 mol %	HCP	$\phi_{DTA} = 0.35$ $\phi_p = 0.18$ $\phi_w = 0.47$	$a = 4.4$ $b = 7.7$ $c = 7.4$	1.7		47	

[a] ϕ_{TTA}, ϕ_{DTA}, ϕ_p, and ϕ_w: volume fraction of TTA ions, DTA ions, P(MAA/NIPAM) chains, and water inside the complexes. R_{sph}: radius of spherical micelles of TTA or DTA ions inside the complexes (R_{lit}: literature value[30]). N_{agg}: aggregation number of micelles packed inside the complexes (N_{lit}: literature value[31]).

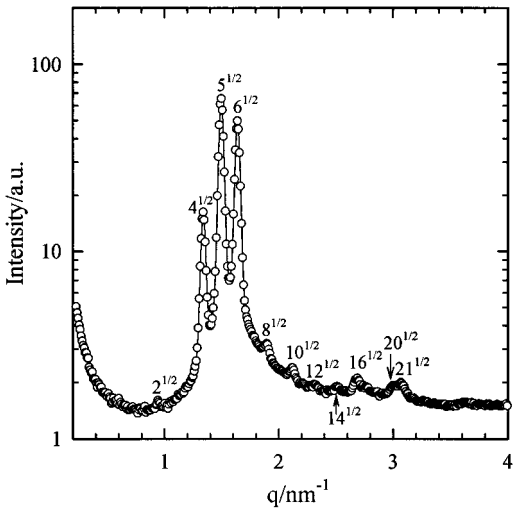

Figure 1. Typical SAXS profile of PMAA gel−TTA complex. The scattered peaks can be indexed according to a cubic structure of *Pm*3*n* space group.

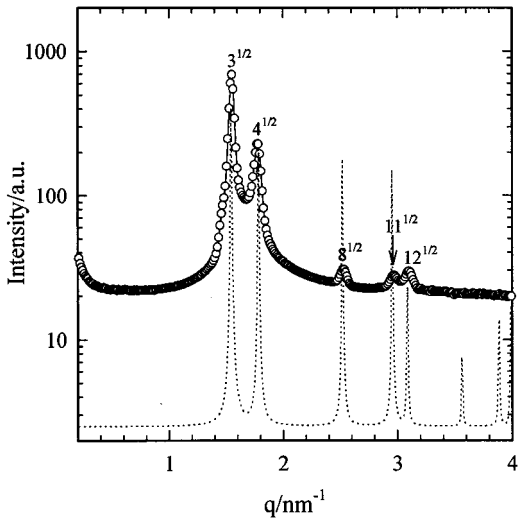

Figure 2. SAXS profile of P(MAA/NIPAM) gel−TTA complex formed with a 67 mol % charge content of the copolymer chains. The dotted line represents the calculated scattering curve based on the FCC close packing of spheres.

charged PMAA chains. More than 10 sharp scattering peaks with a spacing ratio of $2^{1/2}$:$4^{1/2}$:$5^{1/2}$:$6^{1/2}$:$8^{1/2}$:$10^{1/2}$:$12^{1/2}$:$14^{1/2}$:$16^{1/2}$:$20^{1/2}$:$21^{1/2}$ were observed. The extinction rule was compatible with the cubic phase structure of *Pm*3*n* space group, which indicated that the highly ordered structure of the *Pm*3*n* cubic was formed within the collapsed gel. The corresponding diffraction planes could be indexed as 110, 200, 210, 211, 220, 310, 222, 321, 400, 420, and 421. The lattice parameter of the cubic unit cell was calculated to be $a = 9.37$ nm. The *Pm*3*n* cubic phase structure has been found to be located between the aqueous micellar solution and the hexagonal phase (H_α) in many surfactant/water binary or surfactant/water/oil ternary systems.[12−14,27,28] However, it was, for the first time, observed in polyelectrolyte−surfactant complexes. The detailed analysis for the *Pm*3*n* cubic structure has been described elsewhere.[29]

It should be mentioned that the complexes of PAMPS gel−APCl might also show the *Pm*3*n* cubic structure even though only the three most intense peaks indexed as 200, 210, and 211 were observed by Okuzaki and Osada.[9] The proposed structure model, namely, each corner of the primitive cubic lattice was occupied by a sphere that was formed by the large aggregates of bilayer surfactants with paraffin chains both inside and outside the sphere, can be clearly ruled out. First, in terms of the primitive cubic structure, the observable peaks of 100 and 110 should fall within their experimental *q* range; furthermore, these two peaks (100, 110) should be more intense than the three reported peaks (200, 210, and 211). Second, according to the compositions of the PAMPS gel−APCl complexes with 76% water inside, it was unreasonable to assume the hydrophobic tails of surfactants to be widely extended into the water phase.

I.B. Face-Centered Cubic Close Packing of Spheres (FCC). Figure 2 shows the SAXS profile of the P(MAA/NIPAM)−TTA complex at a charge content of 67 mol % in the copolymer chains. Five sharp diffraction peaks with a spacing ratio of $3^{1/2}$:$4^{1/2}$:$8^{1/2}$:$11^{1/2}$:$12^{1/2}$ were observed, indicating a plain FCC structure. The corresponding diffraction planes can be indexed as 111, 200, 220, 311, and 222. The dotted line in the figure represented the simulation scattering curve based on a model of close packing of spheres positioned at the FCC lattice. All the peak positions matched the model very well, while the intensity at higher *q* range showed some difference between the calculated and experimental curves. The parameter of unit cell *a* was calculated to be 7.0 nm.

I.C. Hexagonal Close Packing of Spheres (HCP). Figure 3 shows a typical 2D SAXS image of the P(MAA/NIPAM)−TTA complex at a charge content of 50 mol %

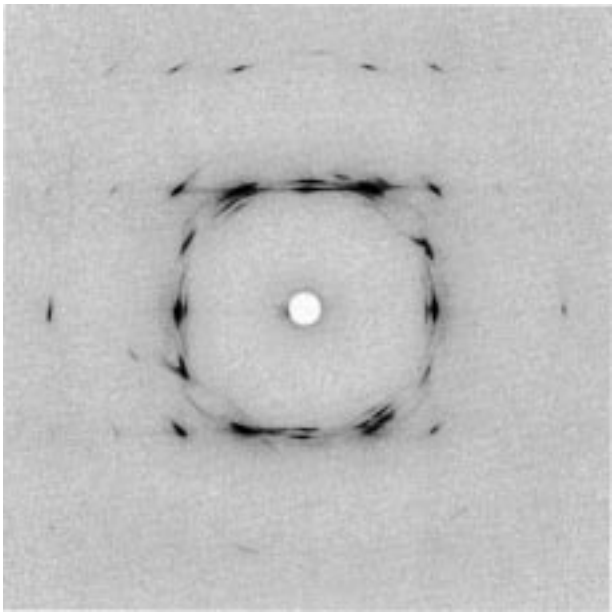

Figure 3. Typical 2D image obtained from the P(MAA/NIPAM) gel−TTA complex formed with charge content of 50 mol % in the copolymer chains. A macrolattice was formed inside the complex.

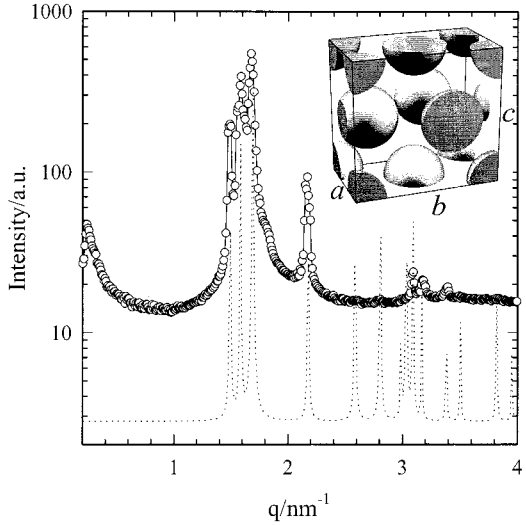

Figure 4. SAXS profile of the P(MAA/NIPAM) gel−TTA complex formed with a charge content of 50 mol % in the copolymer chains. The dotted line represents the calculated scattering curve based on the inset orthorhombic unit cell model for the HCP structure.

in the copolymer chains. A macrolattice was formed inside the complex. The nice scattering picture with reflections from separate crystallites could only be observed when the charge density of the copolymer chains was decreased, probably due to the increase in flexibility of the polyelectrolyte chains when neutral PNIPAM chain became relatively longer. Figure 4 shows the integrated SAXS profile from this nice image; eight scattering peaks were observed. These peaks could be indexed according to the HCP structure. To simplify some calculations for simulating the scattering curve, an orthorhombic unit cell, as shown in the inset of Figure 4, was chosen. Putting one sphere at the origin [0,0,0] and one sphere at the center of the base plane [a/2,b/2,0] produced a single 2D closed-packed layer of spheres. The next layer at $z = c/2$ was identical to the base layer but shifted by b/3 in the y direction.

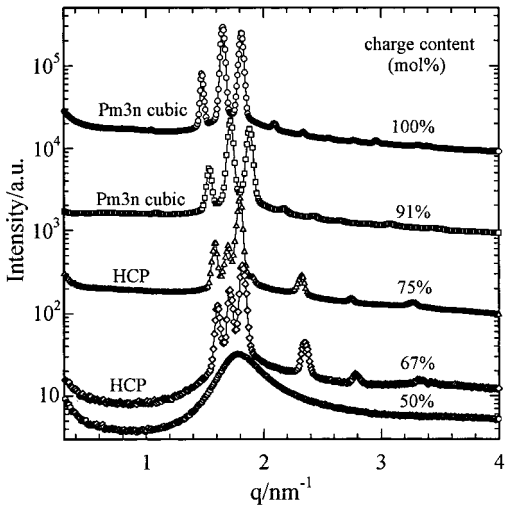

Figure 5. SAXS profiles of P(MAA/NIPAM) gel−DTA complexes at various charge contents of the P(MAA/NIPAM) chains.

The layer at $z = c$ was identical to the one at $z = 0$, resulting in an A−B−A stacking order. Totally, there were four spheres per unit cell. The orthorhombic indexing for the observed scattering peaks was the following: 110 and 020 for 1.49 nm^{-1}, 002 for 1.59 nm^{-1}, 111 and 021 for 1.68 nm^{-1}, 112 and 022 for 2.17 nm^{-1}, 113 and 023 for 2.78 nm^{-1}, 221 and 041 for 3.10 nm^{-1}, 004 for 3.18 nm^{-1}, and 222 and 042 for 3.40 nm^{-1}. The dimension of the orthorhombic unit cell was calculated to be $a = 4.84$, $b = 8.39$, and $c = 7.91$ nm, where a corresponds to the sphere-to-sphere center distance. The dotted line in Figure 4 shows the calculated scattering curve from this unit cell model.

II. P(MAA/NIPAM) Gel−DTA System. Figure 5 shows the SAXS profiles of P(MAA/NIPAM) gel−DTA complexes formed at various charge contents of the P(MAA/NIPAM) chains. At charge contents ≥91 mol %, nearly 10 scattering peaks with a spacing ratio of $2^{1/2}$:$4^{1/2}$:$5^{1/2}$:$6^{1/2}$:$8^{1/2}$:$10^{1/2}$:$12^{1/2}$:$14^{1/2}$:$16^{1/2}$:$20^{1/2}$ were observed. Obviously, the ordered structures formed inside the complexes could be indexed as $Pm3n$ cubic. When decreasing the charge content of the P(MAA/NIPAM) chains to 75 mol %, the structure of the formed complexes changed to HCP in terms of the peak positions. However, the relative intensities of the scattering peaks were different from those of the calculated scattering curve from the HCP unit cell model in Figure 6; namely, the intensity of the second peak (1.70 nm^{-1}) was much lower than that of the calculated scattering curve. It is known that the scattered intensity can be strongly affected by the form factor of a sphere $F(q,R) = \{3/(qR)^3[\sin(qR) - qR\cos(qR)]\}^2$, with R being the sphere radius. The low intensity of the second scattering peak suggested that the first minimum of the form factor function nearly coincided with the position of this peak. This coincidence required that the diameter of the spheres must be about 14% larger than the interdistance between the spheres. It means that the spheres inside the complexes touched each other and were deformed slightly. Therefore, the structure of the complexes could be described as hexagonal close packing of large deformed spherical micelles. The complex formed with 67 mol % charge content of the P(MAA/NIPAM) chains showed a similar HCP structure, but the relative intensities of the scattering peaks were closer to those of the calculated curve from the plain

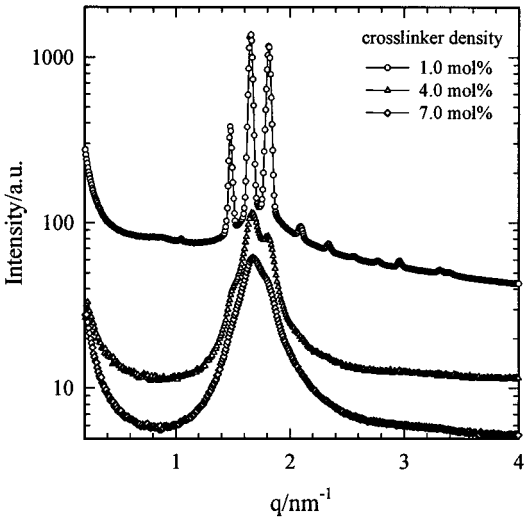

Figure 6. SAXS profiles of PMAA gel−DTA complexes formed at different cross-linker densities of the PMAA gel network.

HCP structural model in Figure 6. The reason was that the spherical micelles became smaller when the charge density of the copolymer chains was decreased so that the spherical micelles did not deform too much. By further decreasing the charge content of the copolymer chains to 50 mol %, only one broad peak was observed, indicating a less-ordered structure inside the complexes.

After having analyzed the compositions and the structures of the complexes, we can clarify the arrangement of the polyelectrolyte chains, the TTA or DTA cations, and water inside the complexes. There was still a great deal of water (i.e., $\phi_w > 0.44$) inside the complexes even though the anionic gel had reached the collapsed limit. Thus, the distribution of water and paraffin chains (hydrophobic components) should be of type I; namely, the paraffin chains were inside the cylindrical and/or spherical micelles, while water stayed outside. The continuous P(MAA/NIPAM) copolymer network chains could be mainly distributed in the water matrix, but close to the polar surface of the spherical and cylindrical micelles so that these micelles could be stabilized by the electrostatic interaction. The copolymer network chains might also be partially distributed at the polar/apolar interface of the spherical and/or cylindrical micelles. The charged groups of the copolymer chains could stabilize the arrangement of the polar headgroups of surfactants in the micelles by electrostatic interactions. Meanwhile, the hydrophobic components (polymer backbone or side groups) could interact with the paraffin chains of the surfactants to stabilize the micelles.

We can further calculate the size and the aggregation number of the micelles packed inside the complexes. For *Pm*3*n* cubic, the distribution of the TTA (or DTA) cations between the rods and the spheres was unknown. Here, we just calculated for the micelles inside the two relatively simple structures of FCC and HCP, both of which consisted of only spherical micelles. For the FCC structure, there are four spheres per unit cell. Thus, ϕ_{TTA} can be calculated as follows

$$\phi_{TTA} = [4(4\pi/3)(R_{sph})^3]/a^3 \quad (1)$$

By knowing the ϕ_{TTA} and a values, R_{sph} could be calculated. Meanwhile, we can calculate the number density of micelles inside the complexes as

$$\rho = 4/a^3 = 1.17 \times 10^{19}\ (1/cm^3) \quad (2)$$

ρ can also be calculated from the TTA concentration C_{TTA} (w/v) inside the complex, the micellar aggregation number N_{agg}, and the molecular weight of TTA ions (M_{TTA}) according to the equation

$$\rho = C_{TTA}N_A/(N_{agg}M_{TTA}) \quad (3)$$

where N_A is the Avogadro number. The combination of eqs 2 and 3 can give N_{agg} as

$$N_{agg} = C_{TTA}N_A a^3/(4M_{TTA}) \quad (4)$$

Thus, by knowing C_{TTA} and a, N_{agg} could be calculated. Similarly, based on the orthorhombic unit cell with four spheres for the HCP structure, we can get the following relations

$$\phi_{TTA(or\ DTA)} = [4(4\pi/3)(R_{sph})^3]/(abc) \quad (5)$$

$$N_{agg} = C_{TTA(or\ DTA)}N_A(abc)/[4M_{TTA(or\ DTA)}] \quad (6)$$

All of the calculated radius and aggregation numbers of the spherical micelles inside FCC and HCP structures are listed in Table 1. For micelles formed by TTA cations, the radius of 2.0 nm was reasonable in terms of the dimension of the TTA cations. It was also close to the radius of spherical TTA micelles formed in water.[30] The N_{agg} of 63 for the TTA micelles formed inside the complexes was consistent with the value of 66 for TTA micelles formed in water (outside the P(MAA/NIPAM) gel).[31] When the charge density of the P(MAA/NIPAM) chains was decreased to 50 mol %, both the R_{sph} and N_{agg} of micelles decreased. Usually, the addition of electrolyte to a surfactant aqueous solution can lead to a decrease in CMC and an increase in N_{agg} of surfactants.[31,32] However, the complex formation of polyelectrolyte with surfactants occurs highly cooperatively and follows a stringent 1:1 stoichiometry in terms of charges. Therefore, the N_{agg} of surfactant molecules inside the complexes will strongly depend on the charge density of polyelectrolyte chains and the flexibility of the polyelectrolyte backbone chains. The decrease in charge density of the polyelectrolyte chains will decrease the number density of surfactant ions inside the complexes, while the restriction of the flexibility of backbone chains will hinder the bound surfactants aggregating together to form micelles. For micelles formed by DTA cations inside the complexes, both the calculated R_{sph} and N_{agg} of the micelles were in agreement with those of the micelles formed outside the polyelectrolyte gel.[31] It should be emphasized that only the aggregation of the TTA (or DTA) cations to monodisperse spherical micelles was taken into account when calculating the R_{sph} value of micelles. If we considered the shell thickness of the hydrated counterions of the P(MAA/NIPAM) chains and the polydispersity of spherical micelles (i.e., the deformed spheres), the diameter of micelles could be larger than the interdistance of the deformed spherical micelles in P(MAA/NIPAM) gel−DTA complexes (a = 4.4 nm). This quantitatively showed the possibility that the first minimum of the form factor function of a sphere could coincide with the position of the second peak in the scattering curve, which resulted in a low intensity of the scattering peak.

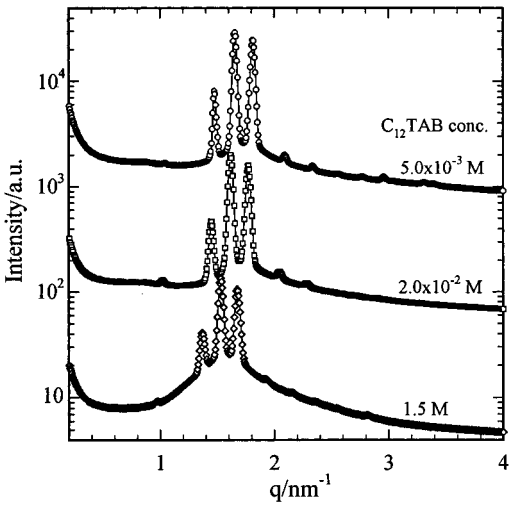

Figure 7. SAXS profiles of PMAA gel−DTA complexes formed at different DTAB solution concentrations (CMC = 1.5×10^{-2} M).

Figure 6 shows the SAXS profiles of the PMAA gel−DTA complexes formed with different cross-linker density of the fully charged PMAA network chains. With increasing cross-linker density of the polymer network chains, the sharp peaks in the scattering curve gradually disappeared. Only one broad peak was observed at a high cross-linker density of 7.0 mol %, indicating that the highly ordered structure inside the complex was disturbed by the high cross-linker density of the polymer network chains. This behavior should be expected since the supramolecular structure was formed inside the 3D gel network and the decrease in mesh size of the polyelectrolyte network would hinder the ordered arrangement of the surfactant molecules inside the gel.

All the complexes discussed above were formed in very dilute surfactant solution (about one-third of the CMC). To examine the concentration effect of surfactant solution, we prepared two complexes formed by fully charged PMAA gels interacting with DTAB solution at concentrations above its CMC. Figure 7 shows the SAXS profiles of PMAA gel−DTA complexes formed in DTAB solution at different concentrations. The ordered structure of *Pm*3*n* cubic inside the complexes remained unchanged even though the complexes were formed at DTAB concentrations much higher than its CMC. However, the corresponding scattering peaks from the complexes shifted to lower q values when the surfactant solution concentration was increased, indicating a larger unit cell. This increase in the interdistance of microdomains was reasonable. As expected, when the complexes were formed in DTAB solution with concentration above CMC, there were more DTAB molecules staying inside the complexes in addition to those DTA cations bound with the PMAA chains. Thus, the aggregation number and the size of the micelles inside the complexes formed at DTAB concentrations above the CMC were larger than those formed at DTAB concentrations much below the CMC. The packing of these large micelles resulted in a larger unit cell inside the complexes.

Conclusions

The interaction of slightly cross-linked anionic polyelectrolyte gels of P(MAA/NIPAM) with oppositely charged surfactants of TTA or DTA salts could produce complexes with very rich highly ordered nanostructures. The charge density variation of polyelectrolyte chains can induce the phase structure transition of the formed complexes. In sequence with decreasing charge density of P(MAA/NIPAM) chains, structures of *Pm*3*n* cubic, FCC, and HCP were, respectively, formed in P(MAA/NIPAM) gel−TTA or (−DTA) complexes. When the charge density of the P(MAA/NIPAM) chains was decreased to some extent, the structures of the resulting complexes became less ordered. The structural elements of spheres and/or rods in these structures were shown to be the spherical and/or cylindrical micelles formed by the self-assembly of TTA or DTA cations inside the complexes, driven by both electrostatic and hydrophobic interactions. Both the aggregation number and the radius of the micelles inside the complexes decreased with decreasing charge density of the polyelectrolyte chains. High cross-linker density of the polyelectrolyte network chains could hinder the formation of highly ordered structure of surfactant molecules inside the complexes.

Acknowledgment. B.C. gratefully acknowledges the support of this work by the National Science Foundation (DMR 9612386) and the U.S. Army Research Office, Durham (DAAG559710022). The use of the SUNY Beam Line (with support from the Department of Energy) at the National Synchrotron Light Source, Brookhaven National Laboratory, is also gratefully acknowledged.

References and Notes

(1) Felger, P. L.; Gadek, T. R.; Holm, M.; Roman, R.; Chan, H. W.; Wenz, M.; Northrop, J. P.; Ringold, G. M.; Danielsen, M. *Proc. Natl. Acad. Sci. U.S.A.* **1987**, *84*, 7413.
(2) Zhu, N.; Liggitt, D.; Liu, Y.; Debs, R. *Science* **1993**, *261*, 209.
(3) Gershon, H.; Ghirlando, R.; Guttman, S. B.; Minsky, A. *Biochemistry* **1993**, *32*, 7143.
(4) Crowell, K. J.; Macdonald, P. M. *J. Phys. Chem. B* **1997**, *101*, 1105.
(5) Ober, C. K.; Wegner, G. *Adv. Mater.* **1997**, *9*, 17.
(6) *Interactions of Surfactants with Polymers and Proteins*; Goddard, E. D., Ananthapadmanabham, K. P., Eds.; CRC Press: Boca Raton, FL, 1993.
(7) Fundin, J.; Brown, W.; Vethamuthu, M. S. *Macromolecules* **1996**, *29*, 1195.
(8) Khokhlov, A. R.; Kramarenko, E. Y.; Makhaeva, E. E.; Starodubtzev, S. G. *Macromolecules* **1992**, *25*, 4779.
(9) Okuzaki, H.; Osada, Y. *Macromolecules* **1995**, *28*, 380.
(10) Chu, B.; Yeh, F.; Sokolov, E. L.; Starodoubtsev, S. G.; Khokhlov, A. R. *Macromolecules* **1995**, *28*, 8447.
(11) Balmbra, R. R.; Clunie, J. S.; Goodman, J. F. *Nature* **1969**, *222*, 11.
(12) Tardieu, A.; Luzzati, V. *Biochim. Biophys. Acta* **1970**, *219*, 11.
(13) Mariani, P.; Luzzati, V.; Delacroix, H. *J. Mol. Biol.* **1988**, *204*, 165.
(14) Lindblom, G.; Rilfors, L. *Biochim. Biophys. Acta* **1989**, *988*, 221.
(15) Auvray, X.; Petipas, C.; Anthore, R.; Rico, I.; Lattes, A. *J. Phys. Chem.* **1989**, *93*, 7458.
(16) Seddon, J. M. *Biochim. Biophys. Acta* **1990**, *1031*, 1.
(17) Khandurina, Yu. V.; Dembo, A. T.; Rogacheva, V. B.; Zezin, A. B.; Kabanov, V. A. *Polym. Sci.* **1994**, *36*, 189.
(18) Yeh, F.; Solokov, E. L.; Khokhlov, A. R.; Chu, B. *J. Am. Chem. Soc.* **1996**, *118*, 6615.
(19) Antonietti, M.; Conrad, J.; Thunemann, A. *Macromolecules* **1994**, *27*, 6007.
(20) Antonietti, M.; Kaul, A.; Thunemann, A. *Langmuir* **1995**, *11*, 2633.
(21) Antonietti, M.; Maskos, M. *Macromolecules* **1996**, *29*, 4199.
(22) Antonietti, M.; Burger, C.; Effing, J. *Adv. Mater.* **1995**, *7*, 751.

(23) Antonietti, M.; Radloff, D.; Wiesner, U.; Spiess, H. W. *Macromol. Chem. Phys.* **1996**, *197*, 2713.
(24) Sokolov, E. L.; Yeh, F.; Khokhlov, A. R.; Chu, B. *Langmuir* **1996**, *12*, 6229.
(25) Brazel, C. S.; Peppas, N. A. *Macromolecules* **1995**, *28*, 8016.
(26) Chu, B.; Harney, P. J.; Li, Y.; Linliu, K.; Yeh, F.; Hsiao, B. S. *Rev. Sci. Instrum.* **1994**, *65*, 597.
(27) Eriksson, P.; Lindblom, G. *J. Phys. Chem.* **1985**, *89*, 1050.
(28) Eriksson, P.; Lindblom, G.; Arvidson, G. *J. Phys. Chem.* **1987**, *91*, 846.
(29) Zhou, S. Q.; Yeh, F.; Burger, C.; Chu, B. Proceedings of the 50th International Symposium on Polyelectrolyte, Japan, 1998.
(30) Berr, S. S.; Caponetti, E.; Johnson, J. S., Jr.; Jones, R. R. M.; Magid, L. T. *J. Phys. Chem.* **1986**, *90*, 5766.
(31) Roelants, E.; De Schryver, F. C. *Langmuir* **1987**, *3*, 209.
(32) Chu, D.; Thomas, J. K. *J. Am. Chem. Soc.* **1986**, *108*, 6270.

MA9810058